Effect of Nutrient Diffusion and Flow on Coral Morphology

Jaap A. Kaandorp,[1] Christopher P. Lowe,[2] Daan Frenkel,[3] and Peter M. A. Sloot[1]
[1]*Parallel Scientific Computing and Simulation Group Faculty of Mathematics, Computer Science, Physics & Astronomy, University of Amsterdam, Kruislaan 403, 1098 SJ Amsterdam, The Netherlands*
[2]*Computational Physics, Faculty of Applied Physics, Delft University of Technology, Lorentzweg 1, 2628 CJ Delft, The Netherlands*
[3]*FOM Institute for Atomic and Molecular Physics, Kruislaan 407, 1098 SJ Amsterdam, The Netherlands*
(Received 26 March 1996)

We describe a method for modeling aggregation in a flowing fluid. In the model, aggregation proceeds by the accumulation of a "nutrient." The nutrient is modeled using a lattice Boltzmann model of transport. The aggregate absorbs the nutrient, and the amount absorbed determines the local growth probability. This model contains some of the essential features of growth of stony corals. We find that the morphology of the aggregates changes drastically as we increase the Péclet number from a regime where nutrient transport is diffusion controlled to a regime where hydrodynamic transport dominates. This is in qualitative agreement with the morphogenesis of stony corals. [S0031-9007(96)01149-0]

PACS numbers: 87.10.+e, 47.20.Hw

In the development of many biological systems, the distribution of chemical agents and nutrients plays a fundamental role. For filter-feeding marine sessile organisms, such as stony corals, the growth process is affected by the distribution of suspended material in the external environment [1]. In most studies only the effect of diffusion is included. However, in many cases one would expect that the influence of flow on the nutrient distribution will be important. In the case of marine organisms, for instance, the nutrients are fairly large suspended particles that have a small diffusion coefficient. In such cases, a modest flow should be enough to dominate the nutrient distribution. From the biological literature [2] it is well known that water movement may have a strong impact on the shape of stony corals. It is often possible to correlate growth forms of stony corals with the amount of water movement. Compact growth forms are generally found under conditions with a large exposure to water movement, while the growth form changes gradually into a branching shape when the amount of water movement decreases [2]. In Fig. 1 three growth forms of the stony-coral species *Pocillopora damicornis* are shown. The compact form in 1(a) originates from an exposed site, the intermediate form 1(b) from a semiprotected site, and 1(c) was collected from a sheltered site.

In this Letter we wish to consider the effect of fluid movement on growth by aggregation. Our approach is to extend, in a fairly straightforward way, the diffusion limited aggregation (DLA) model introduced by Witten and Sander [3]. In DLA the cluster grows by accumulating particles that move purely by diffusion. Warren *et al.* [4] developed an aggregation model in which growth is controlled by the flow velocity in the immediate vicinity of the aggregate. We consider a system in which particles (the "nutrient") are carried to the aggregate by a combination of both flow and diffusion. The relative importance of these two effects on nutrient transport can be characterized by the Péclet number (Pe) defined by $\mathrm{Pe} = \frac{\overline{u}l}{D}$, where $\overline{u}$ is the mean flow velocity, l a characteristic length, and D the diffusion coefficient of the nutrient. A low value of the Péclet number indicates that particles move mainly by diffusion, and a high value indicates that their motion is dominated by flow. By calculating the distribution of nutrient particles in the fluid, we can model the growth

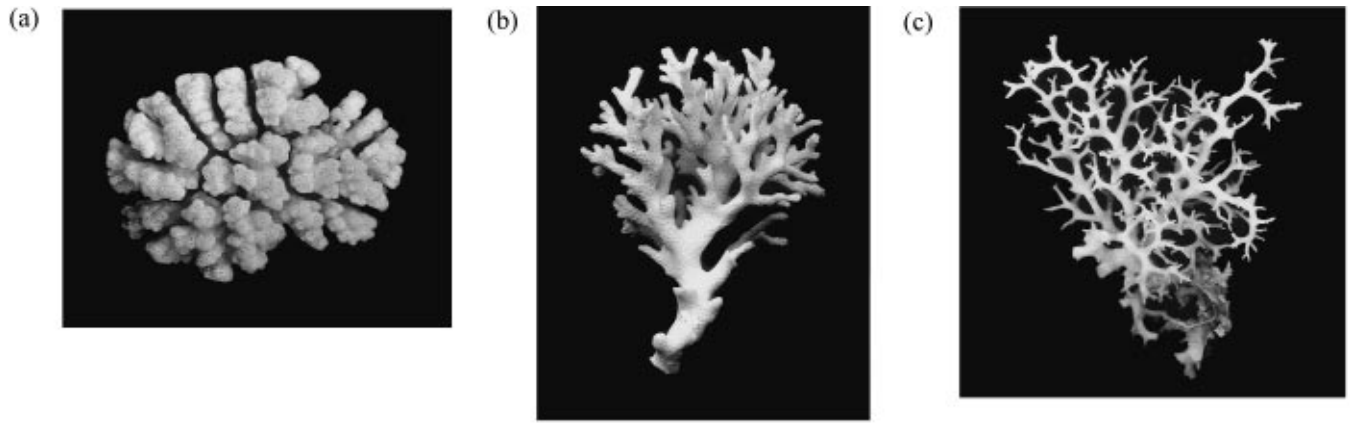

FIG. 1. Growth forms of the stony coral *Pocillopora damicornis* [2]. Form (a) originates from an exposed site, (b) from a semiprotected site, and (c) from a site sheltered from water movement.

 0031-9007/96/77(11)/2328(4)$10.00

of an aggregate which "accumulates" this nutrient. By varying the Péclet number for the system, we can examine the effect, on the aggregation process, of moving from the diffusion-dominated (DLA) regime to the flow-dominated regime. It is also possible to measure the absorption characteristics of the aggregate, which can in turn be used to quantify certain biological properties—for example, the effectiveness of the growth form for catching food.

We modeled the fluid flowing around the aggregate by a lattice Boltzmann equation [5]. The reasons for choosing this approach are threefold: the method is suitable for dealing with flows around complex objects [6], it is straightforward to model nutrients as "tagged" lattice gas particles [7], and finally it is suitable for parallel computation [8]. The lattice Boltzmann model is a preaveraged version of a simple model fluid, the lattice gas. The state of the Boltzmann fluid is specified by the average number of particles with velocity $\mathbf{c}_i$, at each link, which we denote $n_i(\mathbf{r}, t)$. The system evolves subject to propagation and collision. The time evolution of the distribution functions n_i is described by the discretized analog of the Boltzmann equation. Tagged particle motion in the lattice Boltzmann system can be treated as follows. The probability that a particle moves with a velocity $\mathbf{c}_i$ after a collision is given by $n_i(\mathbf{r}, t)/\rho(\mathbf{r}, t)$, where $\rho(\mathbf{r})$ is the total number of particles at the node. The idea is to make use of this fact and propagate in time a quantity $P(\mathbf{r}, t)$, defined as the probability that a tagged particle occupies a site $\mathbf{r}$ at time t. By introducing tagged particles that are identical to the particles constituting the lattice Boltzmann fluid, *but* which have a probability $\Delta/\rho(\mathbf{r}, t)$ of remaining at the same lattice site, it is also possible to vary the diffusion coefficient of the tracer. The time evolution of $P(\mathbf{r}, t)$ for tracer particles which are completely absorbed at the solid/fluid interface is as follows:

$$P(\mathbf{r}, t+1) = \sum_{i \neq i_b}^{b} \frac{[n_i(\mathbf{r} - \mathbf{c}_i, t) - \Delta/b] P(\mathbf{r} - \mathbf{c}_i, t)}{\rho(\mathbf{r} - \mathbf{c}_i, t)} + \Delta \frac{P(\mathbf{r}, t)}{\rho(\mathbf{r}, t)}, \quad (1)$$

where the label i_b indicates a boundary link (a link connecting a node in the fluid to a node inside the solid), and b is the number of discrete velocities. The probability Δ can be explicitly related to the diffusion coefficient [7].

In the simulations we have to consider several sets of boundary conditions. The boundary conditions applied for the fluid, at the faces of the simulation box, are simply periodic. At the solid/fluid interface a "no-slip" (or "stick") boundary condition is applied for the fluid but, as we mentioned above, an absorbing boundary condition is used for the tracer. On the faces of the simulation box we used antiperiodic boundary conditions [6] for the tracer (the distribution on the face is effectively duplicated on the other side of the boundary). This means that, while the aggregate feels to some extent the influence of its periodic images on the flow field, it does not feel their effect on the tracer distribution.

The basic model is shown in Fig. 2. The cluster is initialized with a "seed" located on the bottom plane of the lattice. The bottom plane, "the substrate," is positioned on the x-z plane at $y = 1$, while the seed is one lattice site, located in the middle of the bottom plane. In both the cluster and substrate sites solid/fluid boundary conditions are applied. A net flow, directed in the x direction, is generated by applying a uniform force density to the fluid [5]. The magnitude of this force density is varied over the course of the simulation to keep the mean flow velocity $\overline{u}$ constant (otherwise it would be influenced by the size of the aggregate). This in turn fixes the Péclet number. In all cases the Reynolds number was kept very low, so we are in the "creeping flow" regime. The aggregation process proceeds as follows. First a number of steps of the lattice Boltzmann simulation are performed, followed by a number of steps of the tracer evolution. For the latter, tagged particles are released from the source plane, i.e., the value of $P(\mathbf{r}, t)$ in the top plane is set to a constant. The tagged particles are absorbed by the nodes adjacent to the sites in the substrate plane (the x-z plane at $y = 1$) and the aggregate (the latter we term "sink" nodes). The probability that a sink node will be added to the aggregate is determined by the amount of nutrient absorbed in this node, divided by the total amount of absorbed nutrient. By using a stepwise increase in the number of new nodes added, it is possible to generate large clusters without disturbing too much the equilibria, in both the flow and nutrient patterns, around the cluster. Once we have added a new node (or nodes) the entire process is repeated. Of course, in the simulations we want to model a growth process that is slow compared to all other time scales in the system. We therefore required that both the tracer distribution and velocity field were kept close to equilibrium. A few tens of steps of each calculation, for each growth step, was found to be adequate.

The algorithm was implemented in parallel and the simulations carried out on 16 nodes of a distributed memory Parsytec PowerXplorer system (approximately

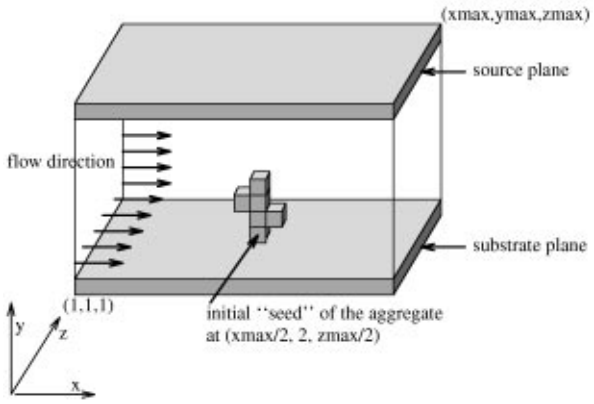

FIG. 2. Basic construction of the aggregate.

TABLE I. The ratio R of total sink nodes to the total cluster size, the 3D fractal dimension D_{box}, the average absorption $\overline{a}$ by the sink nodes of the aggregates, the measure D_{abs} of the uniformity of the nutrient distribution, and the corresponding Péclet numbers Pe of the aggregates.

Pe	0.0150	0.1322	0.2521	0.4918	1.0000	2.0000	2.5000	3.0000
R	2.35 ± 0.10	2.21	1.88	1.64	1.29	1.20	1.31	1.27 ± 0.06
D_{box}	2.27 ± 0.02	2.20	2.27	2.20	2.16	2.10	2.09	2.05 ± 0.04
$\overline{a}$	0.04 ± 0.01	0.85	1.75	3.2	5.5	11.0	13	15 ± 5
D_{abs}	1.7 ± 0.2	1.0	1.0	0.9	0.8	0.7	0.8	0.7 ± 0.1

2 Gflop/s). This allowed us to simulate a system consisting of 144^3 sites. The parallel implementation exploited the nearest neighbor locality of both the LBE and tracer calculation. A detailed time complexity and performance analysis will be presented elsewhere.

The results of the simulations are summarized in Table I. Error bounds on the various quantities we calculated (estimated by repeating the simulations at Pe = 0.0150 and 3.0000 several times) are also given. The ratio R of the total sink nodes to the total cluster size indicates the compactness of the aggregates. The typical cluster size varies between 4×10^4 and 7×10^4. The fractal dimension D_{box} of the surface of the aggregate was determined using a 3D version of the (cube)box-counting method described by Feder [9]. D_{box} measures the space-filling properties of the surface of the aggregate, and has been found to be a useful method for characterizing growth forms. In three dimensions its value varies from a minimum of 2, for a solid object with a perfectly smooth surface, to a maximum of 3 for a solid with a space-filling surface. For us it is more convenient than the common mass scaling exponents because the center of gravity of the cluster changes significantly during growth. The fractal dimension is related to the morphology of the cluster which we illustrate in Fig. 3 by showing slices through the middle of lattice (in the x-y plane). Figure 4 shows the corresponding nutrient distribution. The color shift from black to white in Figs. 4(a) and 4(b) indicates the concentration of nutrient; black indicates the maximum concentration, whereas white areas indicate that the concentration is almost zero.

In the simulations we have determined the number of sink nodes that have a nutrient absorption between a and $a + \Delta a$ for the clusters obtained at the highest and lowest Péclet numbers. The number of sink nodes with absorption rate a, $N(a)$, appears to depend algebraically on a as follows: $N(a) \sim a^{-D_{\text{abs}}}$ so we can determine D_{abs} from a log-log plot. The exponent D_{abs} can be interpreted as a measure of the uniformity of the nutrient distribution. In Table I the average absorption $\overline{a}$ in the boundary nodes, and the values of D_{abs}, are listed for the various Pe numbers. If one considers the pure DLA case, the average absorption would be proportional to the absolute value of the diffusion coefficient (which, for a given geometry, determines the flux of particle arriving at the surface). To facilitate a direct comparison between absorption at different Pe numbers, the values for $\overline{a}$, quoted in Table I, are scaled with the factor $\frac{D_0}{D}$, where D_0 is the value of D we used at the lowest Péclet number.

Figure 3 shows that the overall morphology of the aggregates gradually changes from the DLA-like cluster at Pe = 0.0150 to a much more compact cluster at Pe = 3.0000. The degree of compactness is reflected in the decrease of D_{box} and a decrease of the ratio R (see Table I) with increasing Péclet number. The aggregate at Pe = 0.0150 still differs from "real" 3D DLA. This can be shown, both experimentally [10] and theoretically [11], to give a cluster with a fractal dimension of 2.5. It seems that, even at this low Péclet number, the flow still affects the morphology of the cluster. Figure 3 also illustrates the tendency of the branches of the aggregate to develop towards the origin of the flow. This effect

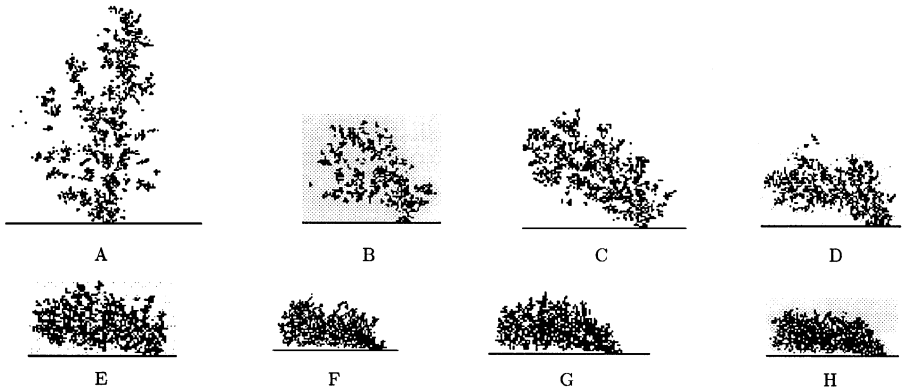

FIG. 3. Slices through the middle (in the x-y plane) of the lattices with the aggregates, the flow is directed from the left to the right. The Péclet numbers for (a)–(h) are given in columns 1–8 of Table I, respectively.

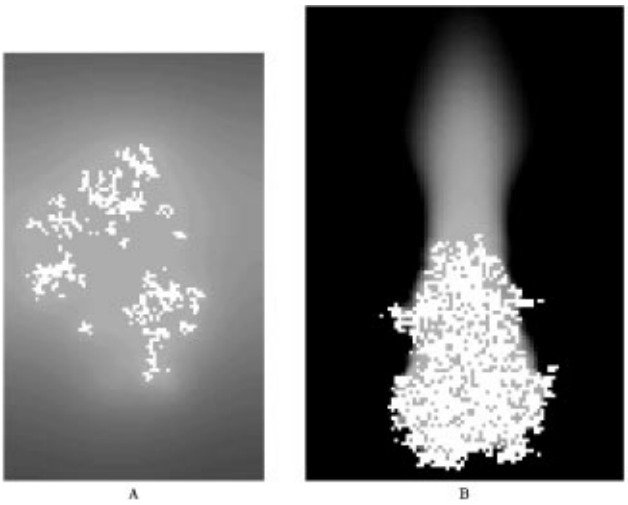

FIG. 4. Slices through the lattice, in the x-z plane. In a and b the nutrient distribution is depicted, for, respectively, Pe [Fig 3(a)] and Pe = 3.0000 [Fig. 3(h)]. In all the pictures the flow is directed from the bottom to the top.

becomes stronger as the flow becomes more important (Pe increases).

The nutrient distributions shown in Figs. 4(a) and 4(b) emphasize the main differences between diffusion and flow dominated regimes. For low Péclet numbers the distribution of nutrient is roughly symmetric about the center of the cluster so there is little asymmetry in the growth process. At higher Péclet numbers a clear asymmetry develops in the distribution with a depleted region developing downstream of the object, while upstream the distribution remains relatively unperturbed by the object. This downstream depletion means there is little probability of growth in the downstream direction, so it is unsurprising that the aggregate develops primarily into the flow. The second point is that, in the immediate vicinity of the cluster, the effect of the flow is to even out variations in the nutrient distribution. At higher Péclet numbers the average absorption increases and the distribution, characteristic of the diffusive regime, changes into a more slowly decaying distribution. In other words, apart from inducing asymmetry, the flow results in a broader distribution of sites being actively involved in the growth process. This is illustrated by the decrease in the measure D_{abs} of the uniformity of the nutrient distribution. This "evening out" of the growth probability between sites appears, in turn, to account for the increasing degree of compactness of the aggregate (reflected by the decrease in D_{box}).

As Table I shows, compared to DLA, the average amount of absorbed nutrient increases with increasing Péclet number. In absolute terms it actually varies surprisingly little. Clearly, the reduction in absorption, due to the reduction in the diffusion coefficient, is approximately offset by the flow moving more material into areas that would otherwise have been significantly depleted. However, nutrient transport to the boundary of the object could still be rather inefficient as far as any organism is concerned (since the flow velocity falls to zero and the nutrient can only ever diffuse to the boundary). This being the case, an efficient use of the nutrient resource, even in a moving fluid, would require some type of active transport mechanism involving nutrient accumulation at some distance from the object.

Our main finding is that the effect of flow on the nutrient distribution is to gradually change the growth form. This contrasts with the conclusion of Warren *et al.* [4]. In their model, fluid flow had little effect on the morphology of the aggregates. The change we observed, from branching to compact structures with increasing water movement, is also exhibited by the stony corals in Fig. 1. Our model is, of course, a simplification. In particular, there is no mechanism present for nutrient accumulation at some distance from the object; in the model the fluid flow is one directional, in reality there is an alternating flow due to the tidal movements; the species *Pocillopora damicornis* also uses photosynthesis for its energy input; there are no effects of erosion included in the model; the actual growth process consists of adding layers of material (varying in thickness) on top of the preceding growth stage, and not explicitly by adding particles. These effects may have varying degrees of importance, but our model does seem to provide the simplest explanation for the trends observed in stony-coral morphology.

This work was carried out within the Massive Parallel Computing pilot project "Portable Parallel Simulation of Crystal Nucleation and Growth" funded by the Nederlandse Organisatie voor Wetenschappelijk Onderzoek (NWO). The simulations were performed on the PowerXplorer from the Interdisciplinary Centre for Complex Computer facilities Amsterdam (IC^3A). The work of the FOM Institute is part of the scientific program of FOM and is supported by NWO. Dr. J. E. N. Veron (Australian Institute of Marine Sciences) kindly permitted us to use the photographs of *Pocillopora damicornis*.

[1] J. A. Kaandorp, *Fractal Modelling: Growth and Form in Biology* (Springer-Verlag, Berlin, New York, 1994).
[2] J. E. N. Veron and Pichon, *Australian Institute of Marine Science Monograph Series Vol. 1, Scleractinia of Eastern Australia Part 1* (Australian Government Publishing Service, Canberra, 1976).
[3] T. A. Witten and L. M. Sander, Phys. Rev. Lett. **47**, 1400 (1981).
[4] P. R. Warren, R. C. Ball, and A. Boelle, Europhys. Lett. **29**, 339 (1995).
[5] A. J. C. Ladd, J. Fluid Mech. **271**, 285 (1994).
[6] A. W. J. Heijs and C. P. Lowe, Phys. Rev. E **51**, 4346 (1995).
[7] C. P. Lowe and D. Frenkel, Physica (Amsterdam) **220A**, 251 (1995).
[8] P. M. A. Sloot, J. A. Kaandorp, and A. Schoneveld, University of Amsterdam, Technical Report No. FWI TR: CS-95-08 (1995).
[9] J. Feder, *Fractals* (Plenum Press, New York, 1988).
[10] P. Meakin, Phys. Rev. A **27**, 1495 (1983).
[11] M. Muthukumar, Phys. Rev. Lett. **50**, 839 (1983).